REPRODUCTION
RESEARCH

Conditional ablation of macrophages disrupts ovarian vasculature

Emily C Turner[1], Jeremy Hughes[3], Helen Wilson[1], Michael Clay[3], Katie J Mylonas[3], Tiina Kipari[3], W Colin Duncan[2] and Hamish M Fraser[1]

[1]*MRC Human Reproductive Sciences Unit, Queen's Institute of Medical Research, Centre for Reproductive Biology,* [2]*Obstetrics and Gynaecology, Division of Reproductive and Developmental Sciences and* [3]*MRC Centre for Inflammation Research, University of Edinburgh, 47 Little France Crescent, Edinburgh, EH16 4TJ, UK*

Correspondence should be addressed to H M Fraser; Email: h.fraser@hrsu.mrc.ac.uk

Abstract

Macrophages are the most abundant immune cell within the ovary. Their dynamic distribution throughout the ovarian cycle and heterogenic array of functions suggest the involvement in various ovarian processes, but their functional role has yet to be fully established. The aim was to induce conditional macrophage ablation to elucidate the putative role of macrophages in maintaining the integrity of ovarian vasculature. Using the CD11b-diphtheria toxin receptor (DTR) mouse, in which expression of human DTR is under the control of the macrophage-specific promoter sequence CD11b, ovarian macrophages were specifically ablated in adult females by injections of diphtheria toxin (DT). CD11b-DTR mice were given DT treatment or vehicle and ovaries collected at 2, 8, 16, 24 and 48 h. Histochemical stains were employed to characterise morphological changes, immunohistochemistry for F4/80 to identify macrophages and the endothelial cell marker CD31 used to quantify vascular changes. In normal ovaries, macrophages were detected in corpora lutea and in the theca layer of healthy and atretic follicles. As macrophage ablation progressed, increasing amounts of ovarian haemorrhage were observed affecting both luteal and thecal tissue associated with significant endothelial cell depletion, increased erythrocyte accumulation and increased follicular atresia by 16 h. These events were followed by necrosis and profound structural damage. Changes were limited to the ovary, as DT treatment does not disrupt the vasculature of other tissues likely reflecting the unique cyclical nature of the ovarian vasculature and heterogeneity between macrophages within different tissues. These results show that macrophages play a critical role in maintaining ovarian vascular integrity.

Reproduction (2011) **141** 821–831

Introduction

Normal ovarian function depends on the cyclical development of follicles followed by ovulation, luteogenesis and luteolysis associated with close regulation of various processes including angiogenesis and tissue remodelling (Redmer & Reynolds 1996, Curry & Osteen 2001). These are primarily regulated by endocrine and paracrine factors; however, complex interactions involving the immune system are well established (Norman & Brannstrom 1994). Macrophages, the most abundant immune cell within the ovary, are derived from blood–borne monocytes. Within tissues, the differentiation of macrophages occurs in response to the surrounding cytokine milieu directing the acquisition of tissue-specific phenotypes (Wu *et al*. 2004). Within the ovary, macrophages have been localised to thecal, luteal and interstitial tissue compartments and in the atretic follicle by specific markers including F4/80 and CD68 in both animal and human studies (Hume *et al*. 1984, Best *et al*. 1996, Petrovska *et al*. 1996, Takaya *et al*. 1997, Duncan *et al*. 1998, Gaytan *et al*. 1998, Li *et al*. 1998). The distribution of macrophages is most abundant in corpora lutea and atretic follicles and fluctuates throughout the ovarian cycle with highest numbers being present at proestrus and metestrus in the mouse strongly indicating hormonal regulation (Brannstrom *et al*. 1993, Petrovska *et al*. 1996). Their specific localisation and dynamic distribution, together with their heterogenic array of functions including phagocytosis, tissue remodelling and cytokine and growth factor release, heavily indicates macrophage involvement in several of the aforementioned ovarian processes (Wu *et al*. 2004); however, their functional role has yet to be established *in vivo*.

In order to further elucidate the physiological role of macrophages within the ovary, conditional macrophage ablation may be employed. Previous attempts by intrabursal injections of clodronate liposomes resulted in partial depletion of thecal macrophages associated with

DOI: 10.1530/REP-10-0327
ISSN 1470–1626 (paper) 1741–7899 (online)
Online version via www.reproduction-online.org

a significant decrease in ovulation rate and apparent inhibition of follicle development (Van der Hoek *et al.* 2000). Furthermore, the osteopetrotic mouse (op/op), which contains a null mutation for colony-stimulating factor 1, an important regulator of macrophage production, displays significantly depleted numbers of ovarian macrophages associated with impaired reproductive efficiency, abnormally long oestrous cycles, reduced ovulation rate and relative inhibition of folliculogenesis (Cohen *et al.* 1997). Despite the achievement of only partial macrophage ablation, both these studies clearly demonstrate the importance of macrophages in regulating normal ovarian function, most notably ovulation and folliculogenesis.

A novel method of macrophage ablation has been achieved by the development of the CD11b-diphtheria toxin receptor (DTR) transgenic mouse in which the expression of human DTR is under the control of macrophage-specific promoter region, CD11b (Cailhier *et al.* 2005). As murine cells are insensitive to DT, macrophages can be selectively and specifically ablated by minute doses of diphtheria toxin (DT) leaving all other cells unaffected. The highly efficient cytotoxic effect of DT is mediated through catalysis of the transfer of an ADP-ribose moiety of NAD^+ onto a histidine residue on elongation factor 2, a polypeptide chain involved in the translation process of protein synthesis, resulting in its inactivation (Saito *et al.* 2001). This is associated with the inhibition of protein synthesis and subsequent macrophage death by apoptosis. This method of macrophage ablation has previously been described in various disease models within the kidney, peritoneum and skin in an effort to increase the understanding of the role of tissue macrophages within inflammatory and healing processes (Cailhier *et al.* 2005, Duffield *et al.* 2005, Mirza *et al.* 2009). Importantly, Cailhier *et al.* (2005) have reported that i.p. injections of DT also resulted in rapid and near complete ablation of F4/80+ cells within the ovary, indicating that this method may have significant advantages over the previously employed clodronate liposome technique. During the course of these studies, it was macroscopically observed that extensive ovarian haemorrhage was present in female mice following DT treatment (J Hughes, unpublished observations). This was unexpected as vascular disruption was not observed in any other tissue.

The indication that a function of macrophages may be in the regulation of ovarian vasculature led us to perform this study to induce conditional macrophage ablation within the ovary in order to elucidate the putative role of ovarian macrophages in maintaining vascular integrity. Another aim is to determine the secondary effects of macrophage ablation on ovarian steroidogenic cells and, finally, attempt to understand why vascular disruption following macrophage ablation is exclusively limited to the ovary.

Results

Effect of DT treatment on ovarian morphology and macrophage localisation

Macroscopically, ovaries of PBS-treated CD11b-DTR mice or DT-treated FVB/nj controls appeared normal (Fig. 1A), although increasing incidence of haemorrhage was observed with time following DT treatment, beginning at 16 h (Fig. 1B). Ovarian sections stained with haematoxylin and eosin (H&E) showed the presence of healthy corpora lutea and luteal tissue from previous cycles in all controls (Figs 1C and 2A). DT treatment of CD11b-DTR mice had no effect on morphology in ovaries collected 2 h following the DT treatment when compared with controls (not shown). By 8 h, there appeared to be focal areas of haemorrhage within the regressing luteal tissue, possibly indicating the early signs of vascular disruption. At 16 h, the changes were striking, with haemorrhage affecting a large proportion of ovarian interstitial and luteal tissue (Fig. 1D). Within the areas of luteal haemorrhage, although some cells showed signs of pyknosis, the majority of cells appeared to be healthy with nuclei retaining morphologically normal appearance (Fig. 2).

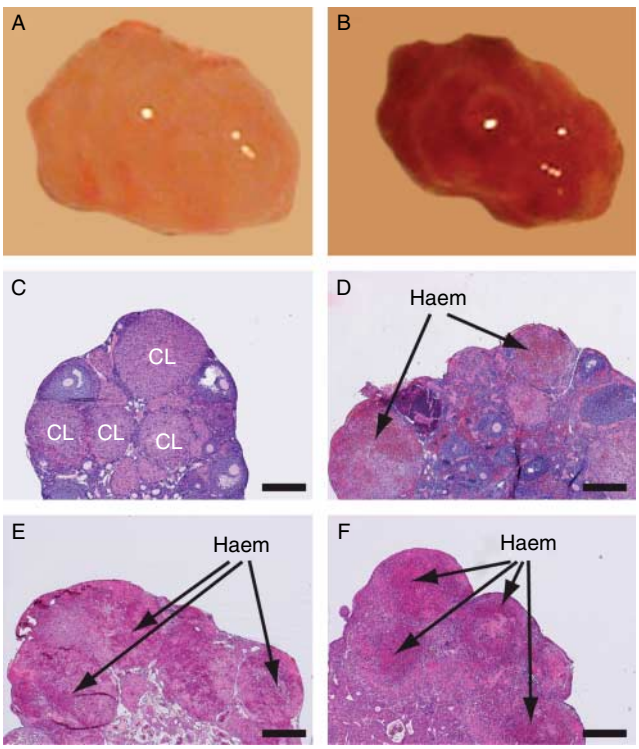

Figure 1 Macroscopic appearance of (A) ovary of control mouse and (B) ovary of mouse 16 h post-DT treatment showing haemorrhagic appearance. (C) H&E section of control ovary demonstrating normal CL with intact cellularity and vasculature. Sections of ovaries 16 h (D), 24 h (E) and 48 h (F) after DT. Note focal regions of haemorrhage (Haem.) at 16 h and extensive haemorrhage at 24 and 48 h. CL, corpus luteum. Bar = 500 μm.

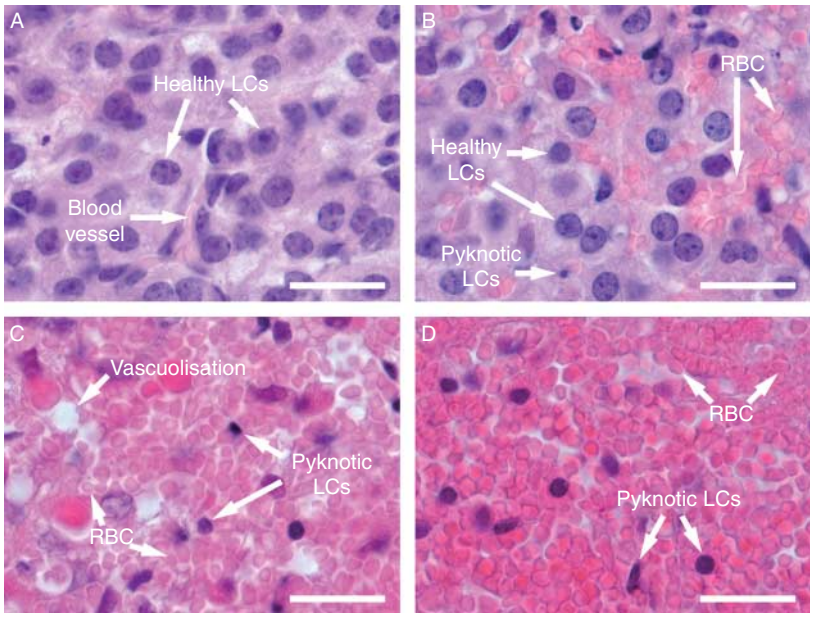

Figure 2 H&E-stained sections showing (A) healthy luteal tissue from control mouse ovary, (B) luteal haemorrhage in 16 h post-DT ovary surrounded by mostly healthy luteal cells, although some pyknotic cells observed, (C) by 24 h, the haemorrhage is more extensive being associated with visible reduction in healthy luteal cells, increased incidence of pyknosis and ovarian necrosis, (D) by 48 h, the extent of haemorrhage has resulted in profound ovarian damage with a dearth of healthy luteal cells. RBC, red blood cells. Bar =20 μm.

At 16 h, haemorrhage within the thecal layer of developing antral follicles was also observed, and the presence of erythrocytes within the granulosa cell layer indicated loss of follicular basement membrane integrity. By 24 h, widespread haemorrhage was observed associated with a marked increase in the density of pyknotic cells and cell vacuolisation indicative of cell death throughout the luteal and follicular tissue (Figs 1E and 2C). By 48 h, the haemorrhage was even more extensive associated with profound damage to ovarian structure, widespread necrosis and vast loss of healthy parenchymal tissue (Figs 1F and 2D). Few distinct ovarian structures could be recognised due to widespread haemorrhagic destruction.

Macrophages stained for F4/80 were observed at varying numbers within the corpora lutea of control ovaries and were often associated with the microvasculature (Fig. 3A). In treated animals, macrophages were absent within the areas of luteal haemorrhage and pyknosis by 16 h (Fig. 3B), although a few were detected in luteal areas which had retained morphologically normal luteal cells (LCs). This was not unexpected as the ablation of macrophages is not 100% in other solid organs (Duffield *et al*. 2005). Macrophages were also present in the thecal layer of developing follicles in control ovaries (Fig. 3C) but were absent by 16 h in treated mice where follicular integrity was lost and haemorrhage was evident (Fig. 3D).

Adrenal glands stained with H&E from treated mice exhibited no apparent differences from controls with no evidence of haemorrhage, whereas after staining with F4/80, a reduction in macrophage numbers was apparent by 16 h (not shown).

Quantification of ovarian haemorrhage

To quantify the extent of haemorrhage, the visualisation of erythrocytes was performed using DAB. In control ovaries, DAB staining was virtually absent, indicating minimal erythrocyte extravasation under physiological conditions (Fig. 4A). Ovaries collected 2 and 8 h following DT treatment showed similar results to controls, whereas ovaries collected at 16, 24 and 48 h exhibited extensive areas of dark brown staining (Fig. 4B). The measurement of percentage area covered by DAB showed statistically significant increases ($P<0.001$) in staining by 16 h compared with earlier time points and control ovaries (Fig. 4C). DAB staining was virtually absent in adrenal glands from both control and treated mice (not shown).

Localisation of ovarian haemorrhage

In order to determine the distribution of haemorrhage within the ovarian compartments, sections from control ovaries and ovaries collected 16 h post-DT treatment were stained with Martius, scarlet, blue (MSB), in which erythrocytes are easily identifiable by their yellow stain (Fig. 5A–F). Statistically significant increases in erythrocyte staining, indicative of haemorrhage, were found in both luteal and follicular regions following DT treatment compared with control ($P<0.001$; Fig. 5G). As expected, due to its highly vascularised nature, luteal tissue represented the region most severely affected by haemorrhage (Fig. 5B–D).

Quantification of endothelial cell area

CD31 staining revealed the dense microvascular tree within the CL of control ovaries (Fig. 6A), whereas by

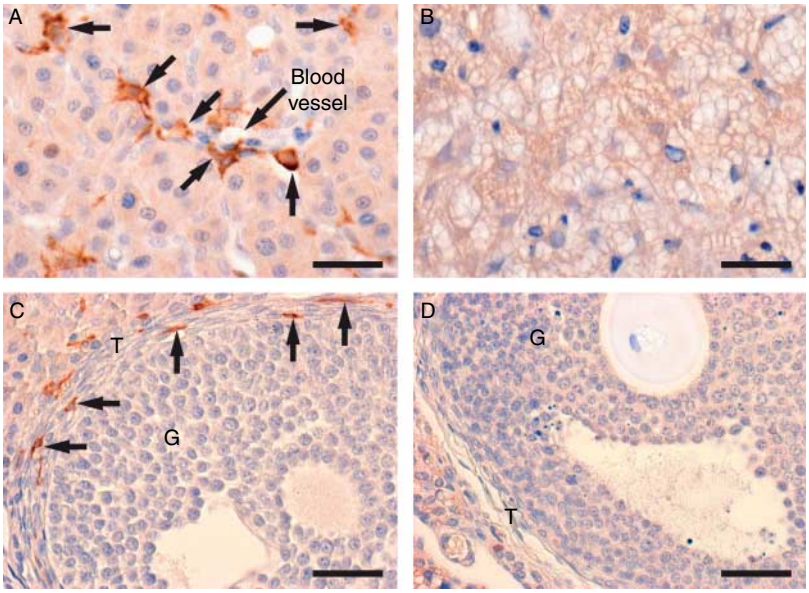

Figure 3 Ovarian sections stained for macrophages by F4/80 showing (A) corpus luteum from control ovary showing healthy luteal cells and the presence of macrophages (brown-staining, black arrows), often associated with blood vessels and (B) a haemorrhagic area of a corpus luteum after 16 h treatment with the absence of F4/80-positive macrophages. (C) Antral follicle from control ovary showing macrophage staining in thecal layer (T) (brown-staining, black arrows). (D) Follicle from a treated animal at 16 h showing absence of macrophages. G, granulosa cell layer. Bar = 20 μm.

16 h after DT treatment staining for CD31 was sparse (Fig. 6B), and by 24 h was replaced by infiltration of red blood cells. Comparison of abundance of CD31 staining revealed a statistically significant depletion of endothelial cells ($P<0.01$) by 16 h in DT-treated ovaries (Fig. 6C). The timing of endothelial cell depletion correlates with the initial observation of ovarian haemorrhage.

Effect of DT on antral follicle health

Using H&E-stained ovarian sections, antral follicles were examined under light microscopy to determine the presence of pyknotic cells within the granulosa cell layer (Fig. 7A–D). The DT treatment adversely affected antral follicle health increasing the proportion of follicles with pyknosis (χ^2) ($P<0.05$). By 16 h following treatment, there was a complete absence of pyknosis free follicles, a reduction that was significant ($P<0.05$) (Fig. 7E). In addition, the presence of antral follicles containing more than 50% pyknotic cells within the granulosa cell layer was only observed at 16 h following DT treatment (Fig. 7D). These changes in follicle health were seen in increasing severity by 24 and 48 h following DT treatment (data not shown). The timing of this increase in granulosa cell pyknosis correlates with the first observation of thecal haemorrhage, indicating that changes in follicle health are likely to be secondary effects of hypoxia due to vascular disruption.

CD11b is expressed exclusively by leukocytes

FACS of digested ovaries from untreated CD11b-DTR mice identified the presence of a small but distinct population of CD11b+ CD45+ cells (upper right

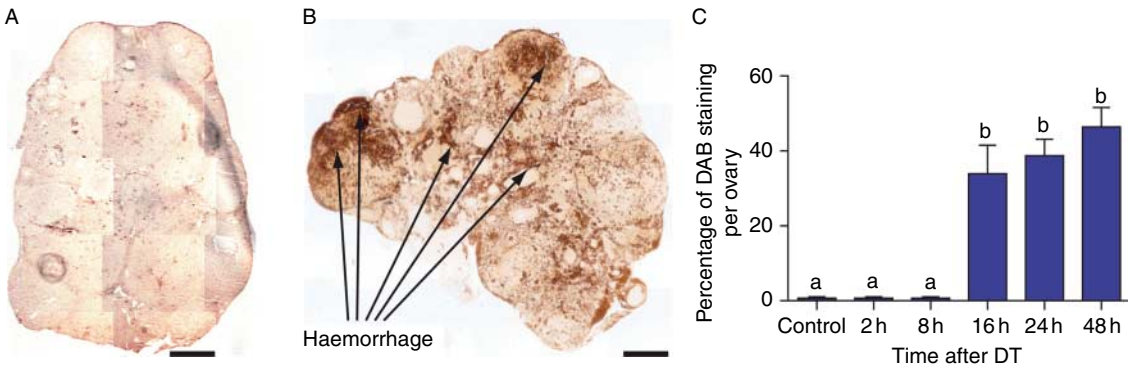

Figure 4 Quantification of haemorrhage in mouse ovaries by DAB staining of erythrocytes. Representative micrographs showing (A) minimal DAB staining of control ovary compared with (B) dark brown staining of erythrocytes (arrows) in 16 h post-DT ovary. (C) Graph to show percentage DAB staining in control ovaries and ovaries collected at intervals post-DT. Data expressed as mean ± S.E.M. Significant difference denoted by different letters. Bar = 350 μm.

quadrant), indicating that the expression of CD11b was limited to cells that are also expressing the pan leukocyte marker, CD45 (Fig. 8). This small population of cells represents macrophages. These results excluded the possibility of ectopic DTR expression by ovarian parenchymal cells.

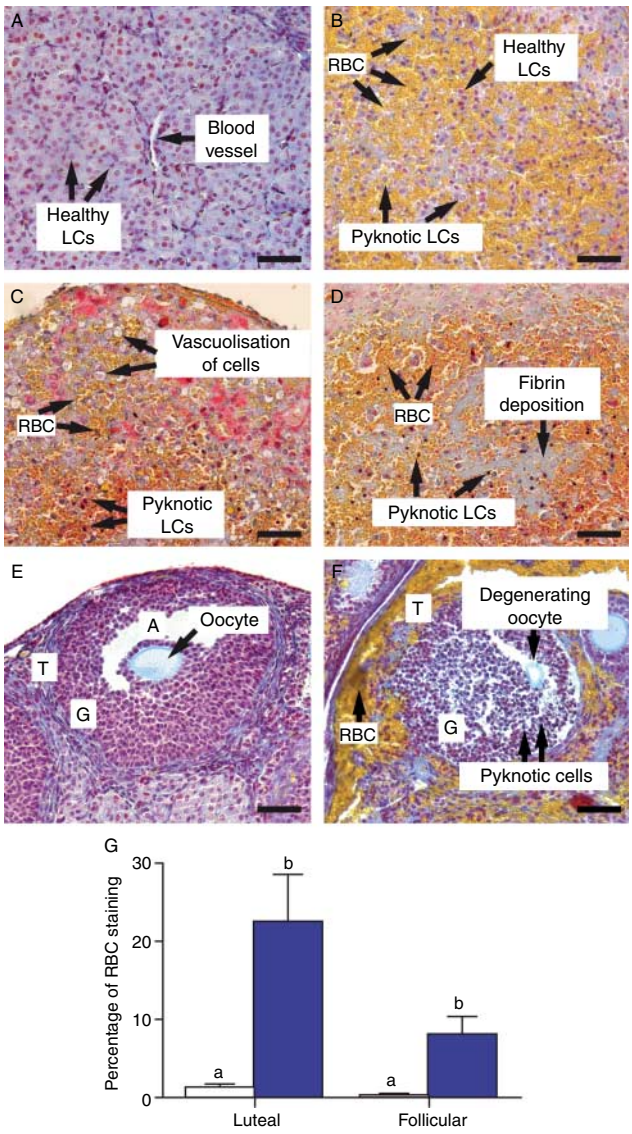

Figure 5 Mouse ovaries stained with MSB, which stains erythrocytes yellow and fibrin blue. (A) Control healthy luteal tissue. (B) Sixteen hour post-DT ovary showing luteal haemorrhage with the presence of pyknotic and healthy LCs. (C) Luteal tissue from 24 h post-DT ovary showing increased haemorrhage and increased disruption of luteal tissue. (D) Forty-eight hours post-DT ovary shows greatest destruction with further increase in haemorrhage, fibrin deposition and virtual absence of healthy ovarian parenchymal cells. (E) Control healthy follicle showing oocyte, antrum (A) and thecal (T) and granulosa (G) cell layers. (F) Follicle from 16 h ovary showing thecal haemorrhage, abundance of pyknotic granulosa cells and degenerating oocyte. (G) Graph of quantification of erythrocyte staining in luteal tissue and within antral follicles in control ovaries and 16 h post-DT. Values are means ±S.E.M. Significant difference denoted by different letters. Bar = 100 μm.

Discussion

Conditional macrophage ablation in CD11b-DTR mice by the administration of DT resulted in extensive haemorrhage affecting thecal and luteal tissue associated with profound ovarian damage and necrosis. Immunostaining for the endothelial cell marker, CD31, confirmed significant associated depletion of these cells. Quantification of the haemorrhage showed luteal tissue to be the most severely affected ovarian compartment, unsurprising due to its highly vascularised nature with endothelial cells representing more than 50% of total cells (Davis *et al.* 2003). Importantly, haemorrhage was not reported in the kidney, peritoneum or skin following the same method of macrophage ablation as reported by Cailhier *et al.* (2005), Duffield *et al.* (2005) and Mirza *et al.* (2009) nor in the adrenal glands of animals in this study. This study proposes that macrophages play a central role in maintaining the integrity of ovarian vasculature.

At 16 h following DT treatment, the areas of both haemorrhagic and unaffected luteal tissue were present; however, after 24 and 48 h, extensive haemorrhage was observed. Staining of macrophages by F4/80 showed that in control ovaries, variable numbers of luteal macrophages were observed, likely related to the age of the corpora lutea, as reported by others (Hume *et al.* 1984, Petrovska *et al.* 1996, Li *et al.* 1998). Crucially, at 16 h, macrophages were absent from haemorrhagic areas confirming macrophage deletion by treatment and its association with the phenomenon of haemorrhage. The haemorrhagic areas were also associated with an increased abundance of pyknotic cells and cell vacuolisation indicative of widespread cell death and necrosis. Similarly, by 16 h, antral follicles within treated ovaries showed signs of pyknotic changes within the granulosa cell layer with some displaying more than 50% pyknotic cells. This degree of pyknosis was not observed in control ovaries suggesting that macrophage depletion causes a progressive increase in granulosa cell atresia beyond what is physiologically normal. Previous studies of ovarian macrophage depletion did not report vascular disturbances; however, this discrepancy may be the result of the differential degree of macrophage ablation. Only partial depletion of the thecal macrophage population was achieved by clodronate liposomes (Cohen *et al.* 1997, Van der Hoek *et al.* 2000), in contrast to the substantial depletion following DT treatment.

Relatively little is known about the functional relationship between the macrophages and the ovarian vasculature. The ovary is unique in being a site of rapid cyclical angiogenesis within the thecal layer and corpus luteum, associated with follicle development and luteogenesis, in contrast to the static nature of the vasculature of other tissues (Fraser & Duncan 2009). Indeed, within the ovary, macrophages are often associated closely with endothelial cells indicating

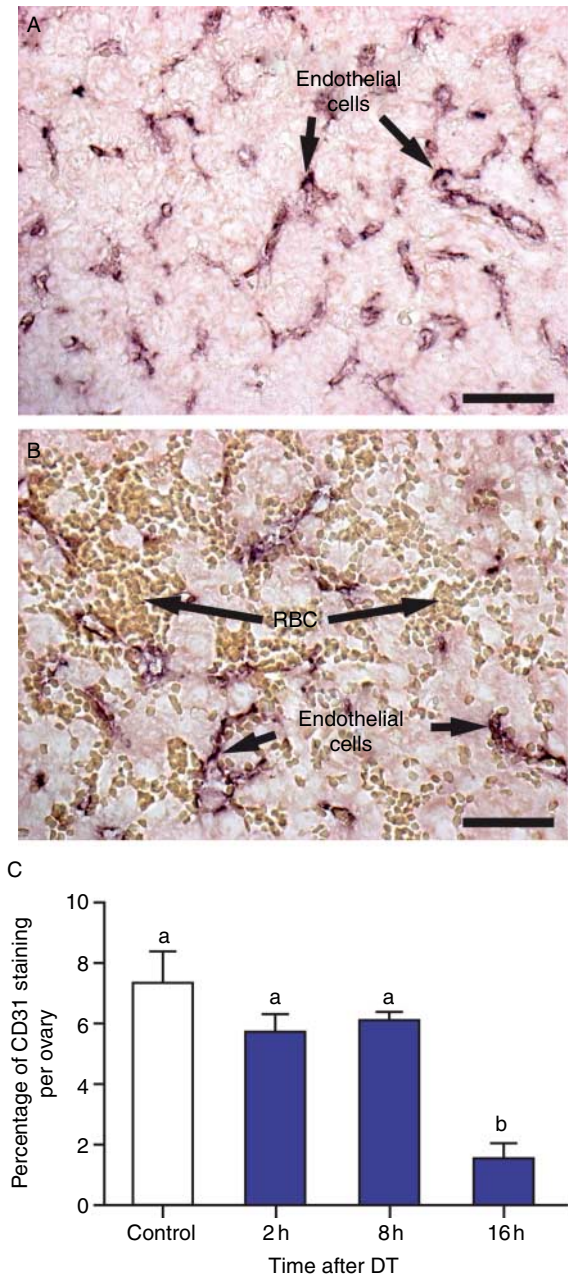

Figure 6 Localisation of endothelial cells in (A) control mouse corpus luteum showing dense CD31-positive staining (reddish brown) and 16 h post-DT ovary (B) with reduced CD31 staining in corpus luteum but increased incidence of red blood cells (RBC) (light brown). (C) Graph showing endothelial cell depletion in corpora lutea following DT treatment. Values are means ± S.E.M. Significant difference denoted by different letters. Bar = 100 μm.

a close functional relationship, as found in this study and as reported previously (Hume *et al*. 1984). Furthermore, during the mid-luteal phase in the human CL, macrophages are abundant around the vasculature (Duncan *et al*. 1998, Gaytan *et al*. 1998). As this represents the period of peak vascular density, it is highly suggestive of macrophages playing a functional role in supporting luteal vasculature, possibly through the release of various cytokines and growth factors or by offering some form of structural scaffold.

The ovary is unique in its ability to undergo cyclic remodelling of the extracellular matrix (ECM), which not only provides structural support but also has a profound effect on regulating normal ovarian processes including ovulation and luteolysis (McIntsuh & Smith 1997, Smith *et al*. 2002). Macrophages are central regulators of ovarian ECM remodelling through the release of various proteases namely matrix metalloproteinases (MMPs) and their inhibitors, tissue inhibitors of metalloproteinases (TIMPs; Wu *et al*. 2004). The ECM both within the vessel wall and surrounding the microvasculature promotes vessel stabilisation by providing both structural support and through activation of various signalling pathways within the endothelium (Davis & Senger 2005, Eble & Niland 2009). Previous studies of DT-induced macrophage ablation within the mouse kidney reported disruption to the MMP to TIMP ratio by a relative downregulation of TIMP1 associated with increased MMP12 activity resulting in enhanced breakdown of collagen III (Duffield *et al*. 2005). This is one possible mechanism through which macrophage ablation may disrupt ovarian vascular integrity; unregulated breakdown and remodelling of the ECM both within the vessel wall and surrounding the microvasculature may result in endothelial disruption and increased breakdown of vessel wall structural proteins. This proposes that macrophages play a physiological role in regulating remodelling of the ECM to promote endothelial support and further enhance vessel stabilisation and maintenance of integrity.

In addition, the haemorrhagic changes following macrophage ablation may be due to the disruption of the putative functional interaction between macrophages and pericytes. Also providing structural support, perivascular pericytes are thought to communicate with the underlying endothelium through gap junctions and by the release of paracrine factors (Bergers & Song 2005). Induced macrophage ablation may result in the disruption of the critical pericyte–endothelium interaction resulting in extensive endothelial dysfunction associated with loss of vascular homoeostasis. Indeed, extensive ovarian haemorrhage occurred in a proportion of rats treated with platelet-derived growth factor (PDGFRβ) receptor blockade due to severe pericyte deficit (Sleer & Taylor 2007), and more extensive results were observed in mice after adenoviral administration of ligand-binding domains of PDGFRβ (Kuhnert *et al*. 2008). The PDGFs are pleiotropic factors released predominantly by endothelial cells and macrophages within the ovary important for the recruitment of pericytes during angiogenesis (Sleer & Taylor 2007). Although it is unlikely that haemorrhage following macrophage ablation was due to PDGF deficiency, it indicates that

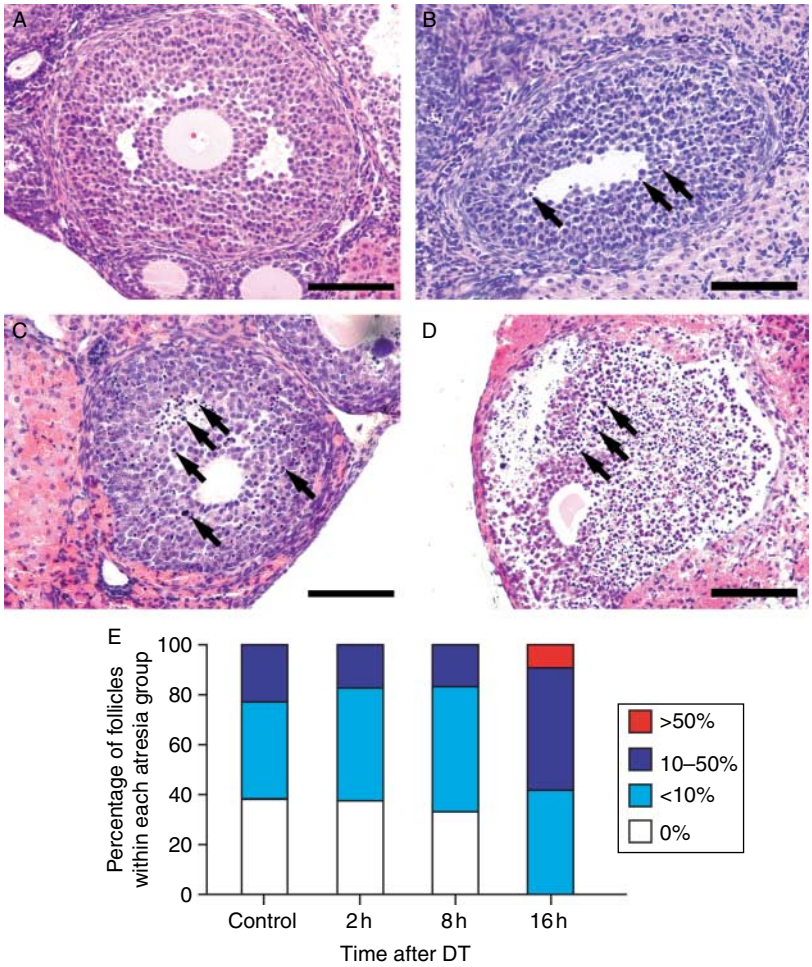

Figure 7 Micrographs of individual antral follicles illustrating different stages of follicle health and changes associated with treatment. (A) Healthy antral follicle with no pyknotic cells, (B) <10% pyknotic cells, (C) 10–50% pyknotic cells and (D) >50% pyknotic cells within the granulosa cell layer as observed 16 h post–DT. Black arrows indicate pyknotic cells. (E) Histogram showing percentages of antral follicles at different degrees of atresia in control ovaries and ovaries collected 2, 8 and 16 h post-DT. DT treatment adversely affected antral follicle health with a complete absence of pyknosis-free follicles by 16 h following treatment ($P<0.05$). Bar =50 μm.

disruption of the pericyte–endothelium interaction would culminate in widespread haemorrhage.

Macrophages have been implicated as important regulators of angiogenesis through the secretion of both pro- and anti-angiogenic factors including vascular endothelial growth factor (VEGF) and basic fibroblast growth factor (Sunderkotter *et al.* 1994, Lamagna *et al.* 2006). Previous studies have reported selective endothelial cell depletion following inhibition of factors involved in the regulation of angiogenesis including inhibition of VEGF in the marmoset corpus luteum during the mid-luteal phase of the cycle (Fraser *et al.* 2006, Fraser & Duncan 2009). Similarly, administration of anti-VEGF antibody in the mouse caused rapid elimination of luteal endothelial cells through detachment from basement membrane (Pauli *et al.* 2005). Importantly, in contrast to this study, no haemorrhage was reported despite endothelial cell loss indicating limited disruption to vessel wall. This finding helps to exclude the possibility that the haemorrhage observed in this study was simply an artefact due to the method of macrophage depletion. It could be hypothesised that the close proximity of supra-physiological numbers of macrophages undergoing apoptosis may simultaneously disrupt the endothelium and cause loss of vessel wall integrity. However, as reported for VEGF inhibition, endothelial cell depletion is not sufficient to cause ovarian haemorrhage (Fraser & Duncan 2009); therefore, other mechanism must be present for macrophage ablation to cause extensive loss of vascular integrity.

Importantly, DT-induced macrophage ablation does not lead to haemorrhagic changes in the kidney, peritoneum, skin (Cailhier *et al.* 2005, Duffield *et al.* 2005, Mirza *et al.* 2009) or adrenal gland. Similarly, administration of anti-VEGF antibody in the mouse did not affect the vasculature of the kidney or liver (Pauli *et al.* 2005). Macrophages show considerable functional and phenotypic heterogeneity between different anatomical locations (Gordon & Taylor 2005). Indeed, as previously mentioned, the ovary is distinct in being a site of cyclical angiogenesis in contrast to the permanent, mature vasculature present in most other tissues including liver and kidney. The immature, dynamic nature of the ovarian vasculature may explain the need for ovarian macrophages to specifically regulate various processes to ensure maximal vascular support. The endometrium also undergoes cyclic angiogenesis, but macroscopically, there were no

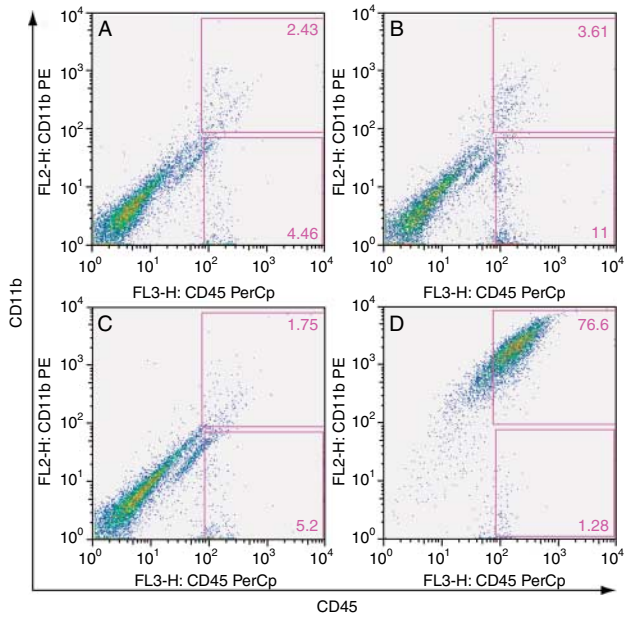

Figure 8 Dot plots of FACS of three pairs of digested ovaries from CD11b-DTR mice. Cells were labelled with PerCp-conjugated anti-CD45 antibody and PE-conjugated anti-CD11b antibody and FACS was performed. (A–C) In digested ovaries, there is a distinct population of CD11b+ CD45+ cells (upper right quadrant). No cells present only expressing CD11b and not CD45 (upper left quadrant). There is a large population of non-leukocyte cells (lower-left quadrant). (D) Digested bone marrow-derived macrophages were used as control and show large population of cells expressing both CD45 and CD11b as expected (upper right quadrant).

indications of haemorrhage in the uterus, although it would be of interest to determine the integrity of the endometrial vasculature in future studies.

In conclusion, conditional macrophage ablation within the ovary results in extensive haemorrhage associated with profound ovarian damage and necrosis. This is the first study to provide evidence that macrophages play a central role in maintaining the integrity of the ovarian vasculature. This may be achieved through close regulation of ECM remodelling to ensure optimal vascular support as well as through interaction with pericytes to regulate the release of various factors to enhance proliferation and survival of underlying endothelium. Secondary effects of macrophage ablation included widespread cell death and necrosis within the ovary, most likely a result of hypoxia following vascular disturbance. The lack of phagocytic clearance of necrotic tissue may further exacerbate ovarian damage through the release of various pro-inflammatory cytokines leading to further structural damage. The unique cyclical nature of the ovarian vasculature and considerable functional heterogeneity between macrophage populations may partly explain why these vascular disturbances are limited to the ovary following macrophage ablation.

Materials and Methods

Transgenic mice

CD11b-DTR mice are transgenic for the human DTR under the control of the macrophage-specific promoter sequence, CD11b. Despite expressing CD11b, granulocyte populations are not affected by DT. Mice are of the FVB/nj background strain. All experiments were performed in accordance with institutional and UK Home Office guidelines. As preliminary observations had indicated that ovarian haemorrhage was present in all treated mice, the animals were not categorised according to the stage of oestrous cycle at treatment.

Macrophage ablation in CD11b-DTR mice by DT administration

Conditional ovarian macrophage ablation was induced in 3-month old female CD11b-DTR mice by i.p. injections of DT (20 ng/g body weight in PBS), while CD11b-DTR control animals were treated with PBS alone. Mice were killed at 2, 8, 16, 24 and 48 h post-DT and 24 and 48 h post-PBS ($n=5$ per group) by cervical dislocation. These time points were chosen to encompass the period surrounding the onset of macrophage cell death that was predicted to be maximal at 8 h (Cailhier *et al.* 2005) and to allow the secondary effects on ovarian morphology to be examined. Ovaries were harvested by dissection, together with adrenal glands for use as control tissue. Right ovaries and adrenal glands were fixed in 10% neutral buffered formalin, whereas left ovaries and adrenal glands were fixed in methyl Carnoy's solution (60% methanol, 30% chloroform and 10% glacial acetic acid). After 24 h, tissue samples were transferred into 70% ethanol before being subsequently embedded in paraffin. Following examination of these tissues, an additional non-transgenic control group was studied following treatment with DT. FVB/nj mice (3-month old) (the background strain for the CD11b-DTR mice) ($n=5$) were injected with DT (20 ng/g body weight in PBS) and ovaries examined after 48 h.

Morphology

To determine the effects on ovarian and adrenal morphology by light microscopy, tissue sections (5 μm) were placed onto BDH SuperFrost slides (BDH, Merck Co., Inc.). The sections were de-waxed in xylene, rehydrated in descending concentrations of ethanol, washed in distilled water and stained with haematoxylin (Richard-Allan, Richland, MI, USA) for 5 min, followed by a wash in water and acetic alcohol before staining with eosin (Richard-Allan) for 20 s. After dehydrating in ascending concentrations of ethanol and xylene, the sections were mounted in Pertex. H&E stain was selected as it best characterised both the gross and subtle changes following DT treatment and enabled differentiation between healthy and regressing luteal tissue and healthy and atretic follicles. Healthy corpora lutea were identified by large eosinophilic cells displaying an organised pattern of arrangement with regressing luteal tissue being distinguishable by cell vacuolisation, reduced cell size and increased disorganisation of the tissue. Antral follicles were recognised by the presence of five or more

granulosa cell layers surrounding the oocytes with or without visible antral cavity (Greenfield *et al*. 2007). The signs of follicular atresia included the presence of pyknotic cells within the granulosa cell layer and detachment of granulosa cells from oocytes (Osman 1985).

Quantification of haemorrhage

To quantify the extent of haemorrhage following DT, two different stains were used. First, diaminobenzidine (DAB) solution was employed for specific erythrocyte staining. DAB, a peroxidase substrate, stains brown the endogenous peroxidase activity within the erythrocytes while leaving other cells unstained (Kuhlmann & Viron 1997). Ovarian and adrenal sections were de-waxed in xylene and rehydrated in descending concentrations of ethanol before being washed with tap water. Vector DAB (Vector Laboratories, Peterborough, UK) (1 drop DAB chromogen per 1 ml DAB buffer solution) was added to the slides for 1 h 15 min. The slides were then washed in water, before being dehydrated by ascending concentrations of ethanol and xylene and mounted in Pertex. Quantitative image analysis was performed using an Olympus BH2 microscope, Spot Insight QE camera and Image-Pro Plus version 4.5 for Windows (Media Cybernetics, Silver Spring, MD, USA). Brown staining areas within the ovary were selected with the mouse pointer to generate a value for total area of positive stain within each section. This value was converted into a percentage by dividing by total area of the ovary and multiplying by 100. The mean percentage positive staining value was calculated.

To further quantify the degree of haemorrhage within specific luteal and antral follicle compartments, formalin-fixed ovarian sections from control and 16 h-treated mice, together with adrenal glands, were stained with MSB. MSB was used as erythrocytes could be clearly identified by yellow staining allowing quantification by image analysis. Unlike DAB, in which no counterstain was used, MSB shows the ovarian structure allowing localisation of the haemorrhage. Image analysis was performed as described earlier to measure the mean percentage yellow staining area within the total luteal tissue and antral follicles.

Immunohistochemistry for F4/80 and CD31

Immunohistochemical staining of macrophages was carried out using the specific marker F4/80 (Hume *et al*. 1984, Petrovska *et al*. 1996, Takaya *et al*. 1997, Li *et al*. 1998, Khazen *et al*. 2005). Methacarn-fixed ovarian and adrenal sections were de-waxed in xylene and rehydrated through descending concentrations of ethanol before being placed in distilled water. To quench endogenous peroxidase activity, the slides were placed in 1.8% hydrogen peroxide (275 ml distilled water and 18 ml of 30% H_2O_2) for 15 min, washed in PBS and placed in Sequenza racks. We sequentially added three drops of avidin, biotin (Avidin/Biotin Blocking Kit, Vector Laboratories, Cat SP-2001) and protein block (DAKO, Cambridge, UK) to the slides, each for 15 min, followed by two washes in PBS (PBS wash omitted following Protein Block). The slides were incubated with primary antibody, rat anti-mouse F4/80 (Invitrogen Ltd), dilution 1:100, overnight at 4 °C. After two washes in PBS, the slides were allowed to stand for 30 min before incubation with secondary antibody, mouse-adsorbed goat anti-rat IgG (Vector Laboratories, Cat number BA4001), dilution 1:200 for 30 min at room temperature. Both the antibodies were diluted with DAKO Antibody diluent. Before staining with DAKO Liquid DAB for 6 min, three drops of Vector ABC (Peterborough, UK) were added for 30 min. The slides were washed in PBS and counterstained with Harris haematoxylin for 20–25 s. After washing in running water, the slides were placed in Scott's tap water for 20–25 s before being returned to running water. For mounting, the slides were placed in xylene and mounted in Pertex. Negative controls included sections in which primary antibody was omitted.

To quantify changes in endothelial cell area, immunohistochemistry for CD31 (platelet endothelial cell adhesion molecule-1) was performed. Formalin-fixed ovarian sections and adrenal glands from 2, 8 and 16 h post-DT mice and respective control mice were de-waxed in xylene and rehydrated as described earlier. Antigen retrieval was performed by incubation in proteinase K (0.625 ml per 50 ml Tris-buffered saline (TBS) for 15 min at 37 °C before being washed in TBS. To reduce non-specific binding, the sections were blocked with normal rabbit serum (NRS, diluted 1:5 in TBS containing 5% BSA) for 30 min followed by three washes with TBS. Both avidin and biotin blocks were employed for 15 min at room temperature each being followed by three washes with TBS. The primary antibody used was CD31 (rat anti-mouse, diluted 1:100 in NRS, BD Pharmingen, Cowley, Oxfordshire, UK, Code No. 553370). Incubation was carried out overnight at 4 °C, followed by three TBS washes, before incubation with the secondary antibody (rabbit anti-rat, biotinylated, diluted 1:500 in NRS) for 30 min at room temperature. After three TBS washes, the slides were incubated at room temperature with ABC AP (Vector AK-5000) prepared 30 min prior to use. After three final TBS washes, the slides were transferred to nitro blue tetrazolium (NBT) buffer containing 5 ml 0.5 M MgCl, 5 ml 1 M Tris/1 M NaCl and 40 ml distilled water. For visualisation, NBT solution, containing 10 ml NBT buffer, 45 ml NBT, 35 ml xyphos and 10 ml levisimole, was then added to the slides for 1 h. The reaction was stopped with tap water, the slides were allowed to air dry, placed in xylene and mounted in Pertex. Image analysis was then performed as described previously (Fraser *et al*. 2006) to calculate the mean area of positive CD31 stain expressed as the percentage of whole ovary area.

Analysis of antral follicle health

To determine the effect of DT treatment on antral follicle health, H&E sections were examined under light microscopy to determine the presence of pyknotic cells within the granulosa cell layer. A semi-quantitative assessment was conducted using the following parameters: i) no pyknotic cells, ii) $<10\%$, iii) between 10 and 50% and iv) $>50\%$ pyknotic cells. The average number of follicles within each parameter was calculated for 2, 8 and 16 h treatment groups and controls. Ovaries treated for 24 and 48 h were not included as extensive structural disruption did not allow comparison with earlier time points.

Flow cytometric analysis

To exclude the possibility of ectopic DTR expression by ovarian parenchymal cells, the flow cytometric analysis (FACS) of digested ovaries from untreated CD11b-DTR mice was performed. To obtain single cell suspensions for FACS, the ovaries were harvested by dissection and chopped into small pieces, before digestion in collagenase B and DNase 1 (1.6 mg/ml collagenase B (Roche), 100 μg/ml DNAse 1 (Ambion, Warrington, UK) in RPMI medium at 37 °C for 45 min with gentle agitation. After centrifugation at 300 ***g*** for 5 min, a further digestion step was carried out with 100 μg/ml DNAse 1 in RPMI medium for 15 min at room temperature. Following centrifugation and re-suspension in 1 ml RPMI, the digested tissue was gently pressed through a 40 μm cell strainer using a flattened pestle and the cell strainer washed with RPMI. The cells were again centrifuged and red blood cells lysed with lysis buffer (Sigma–Aldrich Co.) for 5–10 min at room temperature. The remaining cells were washed in PBS. The single cell suspension of ovarian cells was incubated at 4 °C for 20 min in blocking buffer (10% mouse serum in PBS) followed by staining for 30 min on ice with the antibodies at the appropriate dilution (in PBS, 10% mouse serum) as determined by titration. The antibodies were directly fluorochrome conjugated including anti-CD45-PerCp Cy5.5 (1:100) (BD Pharmingen) and PE-conjugated anti-CD11b (1:100; eBioscience, Hatfield, UK), as well as the appropriate isotype control antibodies, anti-IgG2b-PerCP Cy5.5; (BD Pharmingen) and anti-IgG2b-PE (eBioscience). In total, 100 000 ovarian cells were stained with antibody and underwent flow cytometry with the analysis of 8–10 000 live cell events for each sample. The cells were washed in PBS and fixed in 5% formaldehyde before acquisition and analysis (BD Calibur FACS machine, Oxford and FlowJo, Ashland, OR, USA, software).

Statistical analysis

Significant differences between means were determined by ANOVA and Bonferroni's *post hoc* test. Statistical analysis of haemorrhage quantification within luteal and follicular tissue was performed using unpaired *t*-test. Differences in the proportion of follicles with various categories of pyknotic cells were analysed by χ^2. The number of follicles of each category was analysed by Kruskal–Wallis testing followed by Dunn's pairwise comparison. Statistical differences where $P<0.05$ were considered significant.

Declaration of interest

The authors declare that there is no conflict of interest that could be perceived as prejudicing the impartiality of the research reported.

Funding

This work was supported by the core Grant (U.1276.00.002.00003.01) to Medical Research Council Human Reproductive Sciences Unit to HMF and MRC Grant G070330 to J Hughes. W C Duncan has a Scottish Senior Clinical Fellowship.

Acknowledgements

We thank Mike Millar, Sheila MacPherson and staff of the Histology Core for valuable technical assistance, Prof. F Gaytan, University of Cordoba for advice and Deborah Allen, Ted Pinner and Ronnie Grant for expert help in preparation of figures.

References

Bergers G & Song S 2005 The role of pericytes in blood-vessel formation and maintenance. *Neuro-Oncology* **7** 452–464. (doi:10.1215/S1152851705000232)

Best CL, Pudney J, Welch WR, Burger N & Hill JA 1996 Localisation and characterisation of white blood cell populations within the human ovary throughout the menstrual cycle and menopause. *Human Reproduction* **11** 790–797.

Brannstrom M, Mayrhofer G & Robertson SA 1993 Localisation of leukocyte subsets in the rat ovary during the periovulatory period. *Biology of Reproduction* **48** 277–286. (doi:10.1095/biolreprod48.2.277)

Cailhier JF, Partolina M, Vuthoori S, Wu S, Ko K, Watson S, Savill J, Hughes J & Lang RA 2005 Conditional macrophage ablation demonstrates that resident macrophages initiate acute peritoneal inflammation. *Journal of Immunology* **174** 2336–2342.

Cohen PE, Zhu L & Pollard JW 1997 Absence of colony stimulating factor-1 in osteopetrotic ($csfm^{op}/csfm^{op}$) mice disrupts estrous cycles and ovulation. *Biology of Reproduction* **56** 110–118. (doi:10.1095/biolreprod56.1.110)

Curry TE Jr & Osteen KG 2001 Cyclic changes in the matrix metalloproteinase system in the ovary and uterus. *Biology of Reproduction* **64** 1285–1296. (doi:10.1095/biolreprod64.5.1285)

Davis GE & Senger DR 2005 Endothelial extracellular matrix: biosynthesis, remodeling and functions during vascular morphogenesis and neovessel stabalization. *Circulation Research* **97** 1093–1107. (doi:10.1161/01.RES.0000191547.64391.e3)

Davis JS, Rueda BR & Spanel-Borowski K 2003 Microvascular endothelial cells of the corpus luteum. *Reproductive Biology and Endocrinology* **1** 89. (doi:10.1186/1477-7827-1-89)

Duffield JS, Tipping PG, Kipari T, Cailhier J-F, Clay S, Lang R, Bonventre JV & Hughes J 2005 Conditional ablation of macrophages halts progression of crescentic glomerulonephritis. *American Journal of Pathology* **176** 1207–1219. (doi:10.1016/S0002-9440(10)61209-6)

Duncan WC 2000 The human corpus luteum; remodelling during luteolysis and maternal recognition of pregnancy. *Reviews of Reproduction* **5** 12–17. (doi:10.1530/ror.0.0050012)

Duncan WC, Rodger FE & Illingworth PJ 1998 The human corpus luteum: reduction in macrophages during simulated maternal recognition of pregnancy. *Human Reproduction* **13** 2435–2442. (doi:10.1093/humrep/13.9.2435)

Eble JA & Niland S 2009 The extracellular matrix of blood vessels. *Current Pharmaceutical Design* **15** 1385–1400. (doi:10.2174/138161209787846757)

Fraser HM & Duncan WC 2009 SRB Reproduction, Fertility and Development Award Lecture 2008. Regulation and manipulation of angiogenesis in the ovary and endometrium. *Reproduction, Fertility, and Development* **21** 377–392. (doi:10.1071/RD08272)

Fraser HM, Wilson H, Wulff C, Rudge JS & Wiegand SJ 2006 Administration of vascular endothelial growth factor trap in the 'post angiogenic' period of the luteal phase causes rapid functional luteolysis and endothelial cell death in the marmoset. *Reproduction* **132** 589–600. (doi:10.1530/rep.1.01064)

Gaytan F, Morales C, Garcia-Pardo L, Reymundo C, Bellido C & Sanchez-Criado JE 1998 Macrophages, cell proliferation, and cell death in the human menstrual corpus luteum. *Biology of Reproduction* **59** 417–425. (doi:10.1095/biolreprod59.2.417)

Gordon S & Taylor PR 2005 Monocyte and macrophage heterogeneity. *Nature Reviews. Immunology* **5** 953–964. (doi:10.1038/nri1733)

Greenfield CR, Roby KF, Pepling ME, Babus JK, Terranova PF & Flaws JA 2007 Tumour necrosis factor (TNF) receptor type 2 is an important mediator of TNF alpha function in the mouse ovary. *Biology of Reproduction* **76** 224–231. (doi:10.1095/biolreprod.106.055509)

Hume DA, Halpin D, Charlton H & Gordon S 1984 The mononuclear phagocyte system of the mouse defined by immunohistochemical localisation of antigen F4/80: macrophages of endocrine organs. *PNAS* **81** 4174–4177. (doi:10.1073/pnas.81.13.4174)

Khazen W, M'bika JP, Tomkiewicz C, Benelli C, Chany C, Achour A & Forest C 2005 Expression of macrophage-selective markers in human and rodent adipocytes. *FEBS Letters* **579** 5631–5634. (doi:10.1016/j.febslet.2005.09.032)

Kuhlmann WD & Viron A 1977 Diaminobenzidine cytochemistry in cryo-ultramicrotomy for the detection of peroxidases. *Histochemistry and Cell Biology* **54** 331–337. (doi:10.1007/BF00508275)

Kuhnert F, Tam BYY, Sennino B, Gray JT, Yaun J, Jocson A, Nayak NR, Mulligan RC, McDonald DM & Kuo CJ 2008 Soluble receptor-mediated selective inhibition of VEGFR and PDGFRβ signaling during physiologic and tumor angiogenesis. *PNAS* **105** 10185–10190. (doi:10.1073/pnas.0803194105)

Lamagna C, Aurrand-Lions M & Imhof BA 2006 Dual role of macrophages in tumour growth and angiogenesis. *Journal of Leukocyte Biology* **80** 705–713. (doi:10.1189/jlb.1105656)

Li X-Q, Itoh M, Yano A, Xie Q, Miyamoto K & Takeuchi Y 1998 Distribution of F4/80-positive cells in developing ovaries in the mouse. *Archives of Histology and Cytology* **61** 353–360. (doi:10.1679/aohc.61.353)

McIntush EW & Smith MF 1998 Matrix metalloproteinases and tissue inhibitors of metalloproteinases in ovarian function. *Reviews of Reproduction* **2** 23–30. (doi:10.1530/ror.0.0030023)

Mirza R, DiPietro LA & Koh TJ 2009 Selective and specific macrophage ablation is detrimental to wound healing in mice. *American Journal of Pathology* **175** 2454–2462. (doi:10.2353/ajpath.2009.090248)

Norman R & Brannstrom M 1994 White cells and the ovary- incidental invaders or essential effectors? *Journal of Endocrinology* **140** 333–336. (doi:10.1677/joe.0.1400333)

Pauli SA, Tang H, Wang J, Bohlen P, Posser R, Hartman T, Sauer MV, Kitajewski J & Zimmerman RC 2005 The vascular endothelial growth factor (VEGF)/VEGF receptor 2 pathway is critical for blood vessel survival in corpora lutea of pregnancy in the rodent. *Endocrinology* **146** 1301–1311. (doi:10.1210/en.2004-0765)

Petrovska M, Dimitrov DG & Michel SD 1996 Quantitative changes in macrophage distribution in normal mouse ovary over the course of the estrous cycle examined with an image analysis system. *American Journal of Reproductive Immunology* **36** 175–183.

Redmer DA & Reynolds LP 1996 Angiogenesis in the ovary. *Reviews of Reproduction* **1** 182–192. (doi:10.1530/ror.0.0010182)

Saito M, Iwawaki T, Taya C, Yonekawa H, Noda M, Inui Y, Mekada E, Kimata Y, Tsuru A & Kohno K 2001 Diphtheria toxin receptor-mediated conditional and targeted cell ablation in transgenic mice. *Nature Biotechnology* **19** 746–750. (doi:10.1038/90795)

Sleer LS & Taylor CC 2007 Platelet-derived growth factors and receptors in the rat corpus luteum: localisation and identification if an effect on luteogenesis. *Biology of Reproduction* **76** 391–400. (doi:10.1095/biolreprod.106.053934)

Smith MF, Ricke WA, Bakke LJ, Dow MPD & Smith GW 2002 Ovarian tissue remodelling: role of matrix metalloproteinases and their inhibitors. *Molecular and Cellular Endocrinology* **191** 45–56. (doi:10.1016/S0303-7207(02)00054-0)

Sunderkotter C, Steinbrink K, Goebeler M, Bhardwaj R & Sorg C 1994 Macrophages and angiogenesis. *Journal of Leukocyte Biology* **410** 422.

Takaya R, Fukaya T, Sasano H, Suzuki T, Tamura M & Yajima A 1997 Macrophages in normal cycling human ovaries; immunohistochemical localization and characterization. *Human Reproduction* **12** 1508–1512. (doi:10.1093/humrep/12.7.1508)

Van der Hoek KH, Maddocks S, Woodhouse CM, van Rooijen N, Robertson SA & Norman RJ 2000 Intrabursal injection of clodronate liposomes causes macrophage depletion and inhibits ovulation in the mouse ovary. *Biology of Reproduction* **62** 1059–1066. (doi:10.1095/biolreprod62.4.1059)

Wu R, Van der Hoek KH, Ryan NK, Norman RJ & Robker RL 2004 Macrophage contributions to ovarian functions. *Human Reproduction Update* **10** 119–133. (doi:10.1093/humupd/dmh011)

Received 30 July 2010
First decision 8 September 2010
Revised manuscript received 11 February 2011
Accepted 10 March 2011